Engineering Notes

ENGINEERING NOTES are short manuscripts describing new developments or important results of a preliminary nature. These Notes cannot exceed 6 manuscript pages and 3 figures; a page of text may be substituted for a figure and vice versa. After informal review by the editors, they may be published within a few months of the date of receipt. Style requirements are the same as for regular contributions (see inside back cover).

Monte Carlo Simulation of the Apollo Command Module Land Landing

H. B. CHENOWETH*
North American Rockwell Corporation, Downey, Calif.

Nomenclature

d = confidence limit
L = length of parachute shroud lines
N = normal or load factor
P = probability
SF = structural failure
TF = tumble failure
T = tumble
V = velocity
W = weight
X,Y,Z = coordinate axes
α = probability level associated with confidence limit and structural criteria CFD factor
β = stability contour
γ = soil slope
δ = change in roll angle due to swing velocity
ϵ = ground slope azimuth
θ_0 = contact angle
ϕ = roll, wind azimuth
λ = angle between riser centerline and contact point heat shield angle
μ = difference between wind and ground slope azimuth
Ω = swing angle

Subscripts

A = chute attachment point
C = center of gravity
CM = geometrical origin of command module
H = horizontal
N = normal
R = resultant
T = tangential
V = vertical
W = wind

THE application of a Monte Carlo was developed to determine the land-landing capability of the Apollo Command Module. Should an abort occur within the first few seconds following liftoff of the Saturn V launch vehicle, a probability exists of the Apollo CM drifting back onto the launch complex. The Monte Carlo simulation does not include the probability of drift back to land or of launch pad aborts, nor does it address the problem of couch strut stroke-out dynamics which are coupled nonlinearly with the CM module outer structure. The simulation technique was developed and used as an "after the design" evaluation of the Apollo CM landing capability.

The Apollo CM land-landing system dynamics analysis and simulation process proceeds in three successive stages: 1) the approach to an impeding land-landing of the wind driven CM and parachute system on an arbitrary terrain, i.e., contact conditions, 2) a characterization of the impact loading in terms of the resultant velocity and contact angle, and 3) the failure criteria which are a) the structural allowable statistics of the CM inner structure (because collapse of the inner structure constitutes a hazard to the astronauts on board) and b) the tumbling criterion which determines the probability of the CM tumbling on impact and the probability of a failure (assumed injury to the crew) resulting from the tumbling dynamics.

In the landing loads and criteria analysis, the impact attitude and velocity parameters are used to generate peak loads (including variability), which are then compared with the structural capability of the CM and the simulated failures are counted. The impact attitude parameters are then fed into a tumbling analysis, and the resulting instabilities are compared with post tumbling failure criteria and counted. A condition that would fail more than one criteria is counted as a single failure. At the completion of a set of criterion analysis, a summation of failures is obtained, and the probability of success or failure for land-loading on a given soil is determined.

Command Module Paradynamic Factors

The simulation equations that describe the attitude and velocities of the CM at the instant of impact (Fig. 1) are functions of the environmental and paradynamic parameters. The independent parameters are those defining the attitudes and dynamics of chute descent through the atmosphere (Fig. 2) and the conditions at the impacting surface. Although the parameters pictured vary with time during descent over the range described by their individual CFD's the variation is arrested at impact on a set of random values.

The attitude of the CM parachute system is defined with reference to a set of orthogonal coordinates of which the Z_G axis is vertical to the Earth, positive downward. The horizontal axis X_G is taken as coincident with the wind direction. The attitude of the CM reference axes (X_{CM}, Y_{CM}, Z_{CM}) with respect to the plane through the riser C_L and Z_G is defined by τ and ϕ'. The angle between the Z_{CM} axis and the riser plane projected in the X_G, Y_G plane is designated ϕ. The hang angle τ is computed by calculating a mean value.

$$\bar{\tau} = \tan^{-1}(Z_C - Z_A)/(X_A - X_C) \quad (1)$$

where X_A,Z_A are the chute riser attach point coordinated on the command module and the X_C,Z_C are the vehicle (c.g.,) coordinates. The variance of the hang angle is then computed based on the manufacturing tolerances on the riser attach point and c.g. uncertainty and the CFD is generated. Wind velocity V_H is selected randomly from a CFD generated by wind data taken at Cape Kennedy, the expected impact area.

Land-Landing Velocity and Attitude

The variation of paradynamic factors is arrested at impact on a set of random values. Aligning the $+Z_{CM}$ axis with the wind vector (V_H) and rotating the CM about its X axis results in an angle, i.e., roll angle ϕ'' between the $+Z$ axis and the wind velocity vector and has the form

$$\phi'' = \tan^{-1}[c\tau s\phi'/(c\tau c\Omega c\phi' - s\tau s\Omega)] + \lambda + \delta \quad (2)$$

where c = cosine, s = sine, and $\delta = \tan^{-1}[V_\Omega c\lambda/(V_H + V_\Omega s\lambda)]$ representing the change in roll angle due to chute swing velocity and wind velocity perturbations. Once the vehicle is rolled, it is then pitched about its Y axis by the

Received November 30, 1970; revision received July 15, 1971. This study was supported by NASA Contract NAS9-150. The author wishes to acknowledge the assistance of T. F. Warren in writing this paper and obtaining these results.

* Member Technical Staff and Consultant, Space Division; currently Chief, Litton Systems Inc., Culver City, Calif. Associate Fellow AIAA.

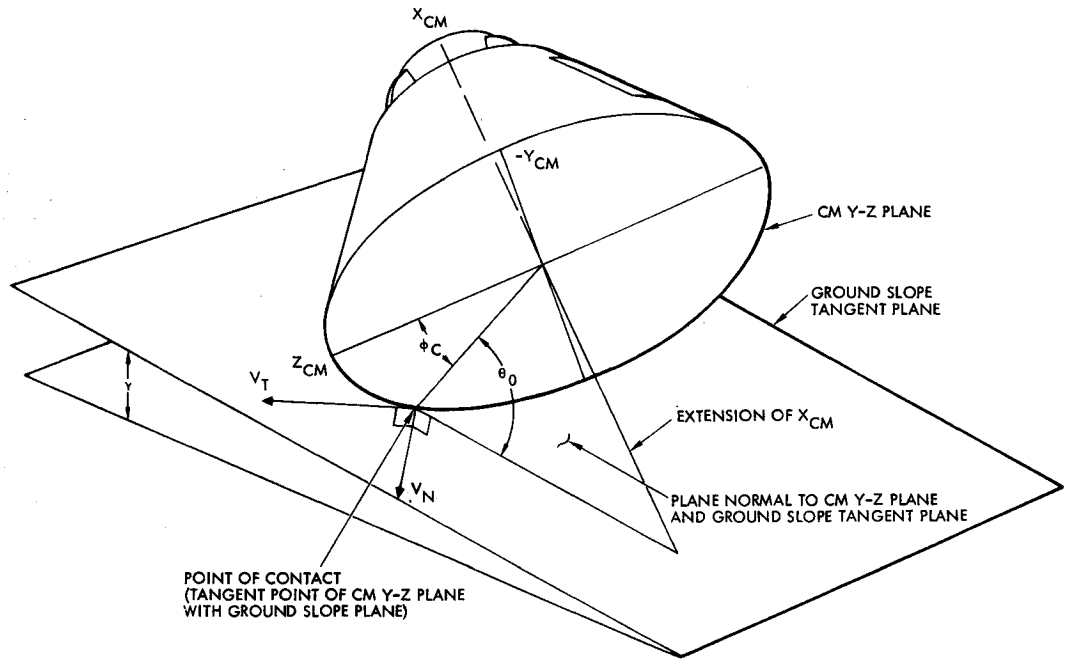

Fig. 1 Description of parameters at initial impact.

hang angle (τ). The contact angle of the vehicle at the instant of impact is then given by

$$\theta_o = \cos^{-1}[C_3 c\gamma + C_4 s\gamma] \tag{3}$$

The ground slope (γ) is derived from a modified NASA ground-slope distribution based on survey data from Cape Kennedy, Fla. Here the contact angle (θ_0) is measured between the CM Y-Z plane, (Fig. 1) and the ground-slope tangent plane in a plane normal to both. The swing velocity (V_Ω) of chutes perturbs the normalized wind velocity (V_h') and the roll angle and is given by

$$V_\Omega = (gLs\Omega \tan\Omega)^{1/2} \tag{4}$$

The normal velocity (V_N) is that component of the resultant CM velocity (i.e., with respect to the center of gravity) normal to the impacting surface. The normal velocity is determined from

$$V_h' = [(V_H + V_\Omega s\lambda)^2 + (V_\Omega c\lambda)^2]^{1/2} \tag{5}$$

also $\mu = \phi_w - \epsilon$, and ϵ is the ground-slope azimuth; ϵ is determined by using a random-number generator (i.e., rectangular distribution).

The wind azimuth (ϕ_w) is based on a wind rose taken at Patrick AFB, Fla., using hourly data compiled and analyzed for February.[5]

$$V_N = V_h' c\mu s\gamma + V_v c\gamma \tag{6}$$

The tangential velocity (V_T) is the velocity component measured in the ground-slope tangent plane and is determined using the following equation:

$$V_T = [(V_h')^2 + (V_v)^2 - (V_N)^2]^{1/2} \tag{7}$$

The angle ϕ_C determines the point of contact of the aft heat shield with the ground at initial impact; as shown in Fig. 2, it is measured in the Y-Z plane of the vehicle from the $+Z$ axis to the point of contact.

$$\phi_C = -\left[\cos^{-1}\left\{\frac{D_1G_1 + D_2G_2 + D_3G_3}{(D_1^2 + D_2^2 + D_3^2)^{1/2}(G_1^2 + G_2^2 + G_3^2)^{1/2}}\right\} - \frac{\pi}{2}\right] \tag{8}$$

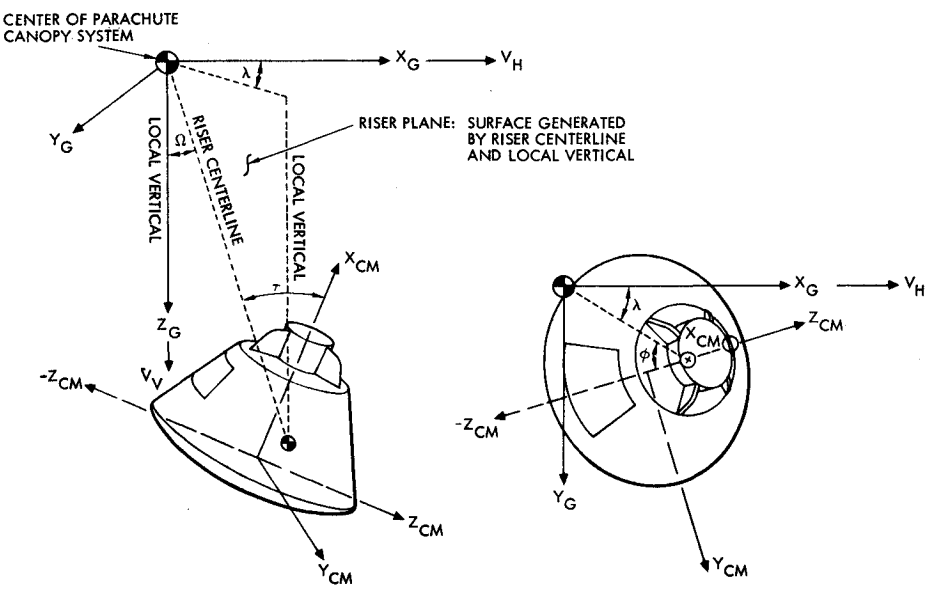

Fig. 2 Parameters describing descent of the CM-parachute system in the atmosphere.

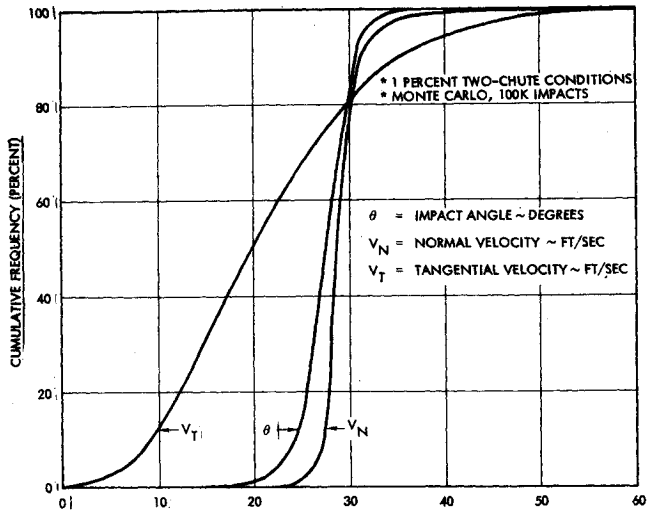

Fig. 3 Command module impact parameter distributions, land-landing.

where

$$D_i = A_i - C_iD_o \qquad i = 1,2,3$$

$$D_o = A_1C_1 + A_2C_2 + A_3C_3$$

$$G_1 = C_3s\gamma s\mu - C_2c\gamma, \quad G_2 = C_1c\gamma - C_3s\gamma c\mu$$

$$G_3 = C_2s\gamma - C_1s\gamma s\mu$$

$$A_1 = c\lambda s\Omega \qquad A_2 = s\lambda s\Omega \qquad A_3 = c\Omega$$

$$Q_1 = s\lambda s\phi' - c\lambda c\Omega c\phi', \qquad Q_2 = c\lambda s\phi' - s\lambda c\Omega c\phi'$$

$$Q_3 = s\Omega c\phi'$$

$$C_i = A_ic\tau + Q_is\tau, \qquad i = 1,2,3$$

$$C_4 = C_1c\mu + C_2s\mu$$

The cumulative frequency distributions of V_N, V_T, and θ are given in Fig. 3.

Land-Landing Loads Analysis

Loads generated by a land-landing are characterized by a phenomenological nonlinear spring model. The CM reacts with the soil dynamically in a composite spring manner dependent on vehicle and soil mass properties, impact attitude and velocity characteristics, and vehicle and soil dynamic properties.[2,6] The CM reaction to initial impact is a simple spring with no initial damping.[2] As the impact continues, the spring deflection coefficient becomes a nonlinear function of contact attitude, velocity, soil, and vehicle dynamic properties. Tests[6-9] have shown that a large percentage of the work done by a command module impacting on an arbitrary ground surface is converted to structural energy during the soil-vehicle interaction. A comparison of drop test load factor results and predicted load factors (correlation = 0.65) is shown in Fig. 4.

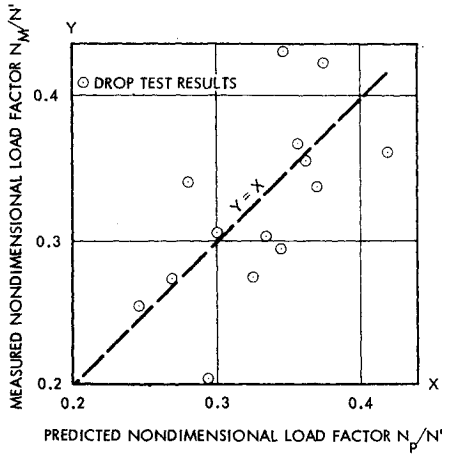

Fig. 4 Measured vs predicted nondimensional impact load factors.

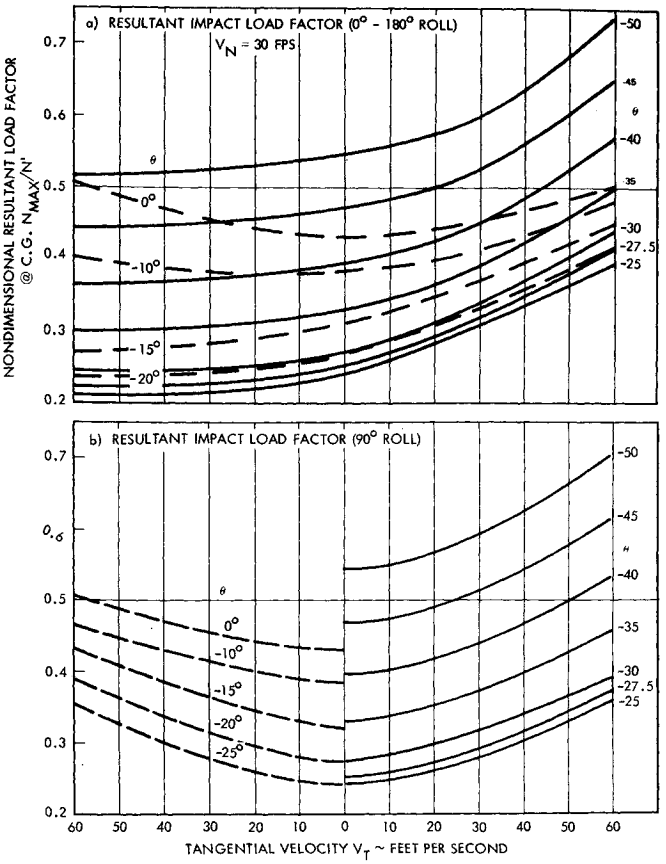

Fig. 5 Resultant impact load factor prediction.

The model results for the predicted load factor is shown for discrete roll angle values of 0°, 180°, and 90° in Fig. 5. The curves in Figs. 4 and 5 are presented as dimensionless variables for ease of computation. The load factor measured value is considered to be more realistic than the model value so a histogram was constructed (based upon the scatter); the cumulative frequency distribution of this scatter is given in Table 1. Values from this CFD are added algebraically to the mean value (N_{MAX}) in the simulation.

Structural Design Criteria and Failure Analysis

In a determination of crew safety, of primary interest is the portion of the command module structure encompassing the crew compartment. This portion is made up of an aft-bulkhead ring at the heat shield and longerons that compose the

Table 1 Dimensionless load factor dispersion cumulative frequency distribution[a]

N/N'	CFD	N/N'	CFD
−0.09375	0.00	0.01166	59.87
−0.09335	2.18	0.02458	69.15
−0.08167	4.01	0.03500	77.34
−0.07000	6.68	0.04667	84.13
−0.05833	10.56	0.05833	89.44
−0.04667	15.87	0.07000	93.32
−0.03500	22.66	0.08167	95.99
−0.02458	30.85	0.09335	97.72
−0.01166	40.13	0.09375	100.00
0	50.00	...	...

[a] Based on North American Rockwell and NASA drop-test results.

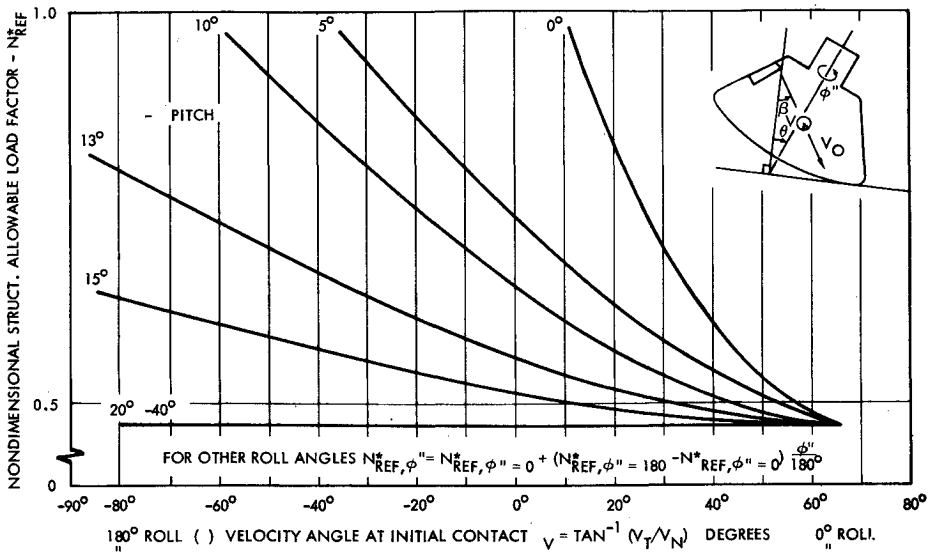

Fig. 6 Structural allowable load factor.

forward and aft assembly primary load paths. The crew compartment 90% structural allowable is presented in Fig. 6. The structural allowable load factor is a function of vehicle roll, contact angle, and normal and tangential velocity for the first peak loading impact. To complete this phase of the simulation, it is necessary to include the variability of the materials about the 90% values shown in Fig. 6. This variability is shown in terms of its cumulative frequency distribution in Table 2 and is determined by $N^* = \alpha N_{\text{Ref}}{}^*$.

Land-Landing Stability Criteria

The tumbling criteria in parallel or series with other land-landing criteria presents a realistic filtering system for determination of the probability of success based on a large number of land impact conditions generated by the paradynamics distributions coupled with other parameter distributions in the simulation. The criteria indicates the limiting stability value of resultant c.g. velocity (V_R) at impact for any contact angle and roll condition of the vehicle on hardpack soil with slopes up to ±15°. If the limiting value of the resultant velocity is exceeded for an impact, the vehicle will tumble. Tumbling may impart intolerable accelerations in the crew extremities in the eyeballs-out direction against their restraint harnesses and could subject the crew to possible injury from detached hardware during tumbling dynamics or cause egress difficulty due to tunnel/sidewall hatch blocking. Many tumbling conditions will not jeopardize crew safety and should not be considered failures. Based upon drop-test results, the crew safety criteria assumed is based on horizontal velocity: 1) 100% tumble failures $V_T \geq 40$ fps; 2) 25% tumble failures, 40 fps $> V_T >$ 20 fps; and 3) no tumble failures, 20 fps $\geq V_T$.

Early in the Apollo program, a few land drop tests were conducted with prototype and scale models. These tests indicated that stability was best at 0° roll and degraded as 180° roll was approached assuming all other impact parameters held constant; empirical results are combined with energy conservation equations in the analysis. During the examination of land-drop test data, it was noted that the limit velocity contours at which tumbling occurred took the general shape of ellipses from 0° to 180° roll and that these conics would best describe the limiting velocity conditions for tumbling (Fig. 7).

Table 2 Structural allowable load factor ratio (α) cumulative frequency distribution

CFD	0	10	30	50	70	80	100
α	1.777	1.102	1.072	1.051	1.030	1.000	0.924

Land-Landing Success Probability

The following equation is used to determine the probability of a successful land landing:

$$P_{\text{success}} = 1.0 - P(SF) - P(TF) + P(TF/SF) \quad (9)$$

The probability terms have been found to have the following approximate ratios:

$$P(SF):P(TF):P(T):P(TF/SF) = 1:31:91:0.36 \quad (10)$$

where $P(T)$ is the probability of tumbling.

The Monte Carlo analysis only approximates the success probability and a determination of the mean or absolute probability of success would require a large number of Monte Carlo samples. An approach to determining the absolute probability of success to utilize the following relationship:

$$P\{|\hat{P}_o - P_o| < d\} = \alpha \quad (11)$$

The relationship states that the probability of success lies within the tolerance or confidence interval (d) with α probability. Assuming that the probability is normally dis-

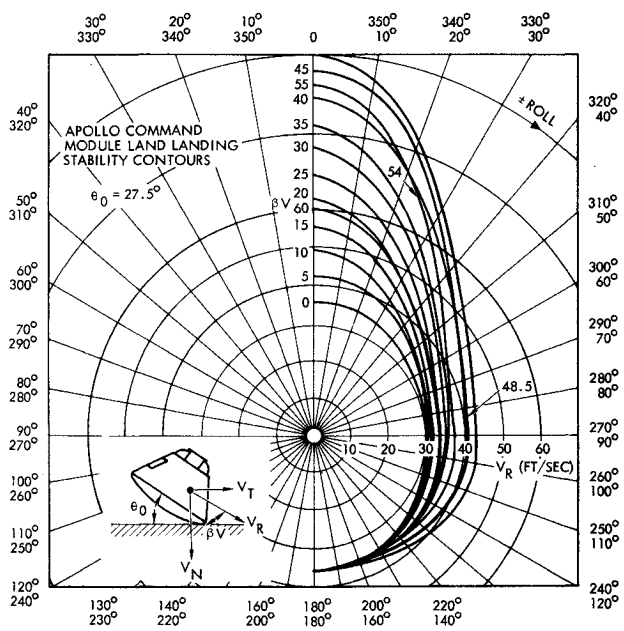

Fig. 7 Apollo command module land-landing stability contours.

tributed about $\hat{P}_o$ yields:

$$P_o - d \leq \hat{P}_o \leq P_o + d \qquad (12)$$

where

$$d = Z\alpha/2[P_o(1 - P_o)/n]^{1/2}$$

and $Z\alpha$ refers to the number of standard deviations in the interval from the mean to $\alpha/2$ (for a 95% probability a normal probability table yields 1.96). For a preselected value of α and a value of P_o from one or more Monte Carlo simulations, the value of confidence limit (d) can be computed using Eq. (12). The computed confidence interval is of the same order of magnitude as $P(TF/SF)$ for large n.

Conclusions

The Monte Carlo simulation of peak loads, tumbling and the determination of the probabilities of success has been achieved through the use of analytical and empirical techniques. This simulation technique can be modified or improved to evaluate the design of CM as better and more refined information becomes available. Since the peak load analysis generates impact loading close to experimental values it can be concluded that the Monte Carlo simulation has adequately simulated land-landing.

References

[1] Mize, J. H. and Cox, J. G., *Essentials of Simulation*, Prentice-Hall, Englewood Cliffs, N.J., pp. 143–147.

[2] Kovalevsky, L., Matthiesen, R. B., and Rish, F. L., "Landing on Earth Media," SD 68-768, Sept. 1968, Space Div., North American Rockwell Corp., Downey, Calif.

[3] Golden, J. T., *Fortran IV Programming and Computing*, Prentice-Hall, Englewood Cliffs, N.J., 1965, pp. 38–40.

[4] Vaughan, W. W., "Cape Kennedy Surface Quasi-Steady State Wind Statistics," R-AERO-Y-63-65, May 1965, NASA Marshall Space Flight Center, Huntsville, Ala.

[5] Smith, J. W. and Smith, O. E., "Surface Wind Statistics for Patrick AFB, Florida," NASA-MSFC Rept. MTP-AERO-61-78, Oct. 1961, NASA Marshall Space Flight Center, Huntsville, Ala.

[6] Reece, L. C. et al., "Investigation of the Effects of Soil Conditions on the Landing of a Manned Spacecraft," Final Rept., March 1964, Structural Mechanics Research Lab., University of Texas, Austin, Texas.

[7] Trotter, J. A., "Land Impact Test Drop No. 47, Accelerometer and Strut Data Report," ATO-T1-63-20-26, Sept. 1963, Space Div., North American Rockwell Corp., Downey, Calif.

[8] Russell, R. H., "Land Impact Test Drop No. 49, Internal Accelerometer and Strut Data Report," ATO-DE-63-20-35, July 1963, Space Div., North American Rockwell Corp., Downey, Calif.

[9] Trotter, J. A., "Land Impact Test Drop No. 25, Accelerometer and Strut Data Report," ATO-TD-64-20-72, Feb. 1964, Space Div., North American Rockwell Corp., Downey, Calif.

Inversion of Spin-Stabilized Spacecraft by Mass Translation— Some Practical Aspects

NORMAN H. BEACHLEY*

University of Wisconsin, Madison, Wis.

INVERSION can be a very useful maneuver for certain types of spin-stabilized spacecraft; e.g., for a satellite whose spin axis is kept parallel to that of the Earth, inversion twice a year would allow the same end to remain in the shade all year round, protecting devices mounted on the spin axis which are sensitive to solar radiation.

Received January 22, 1971; revision received July 12, 1971. This work was supported in part by NASA.

Index category: Spacecraft Attitude Dynamics and Control.

* Assistant Professor of Mechanical Engineering.

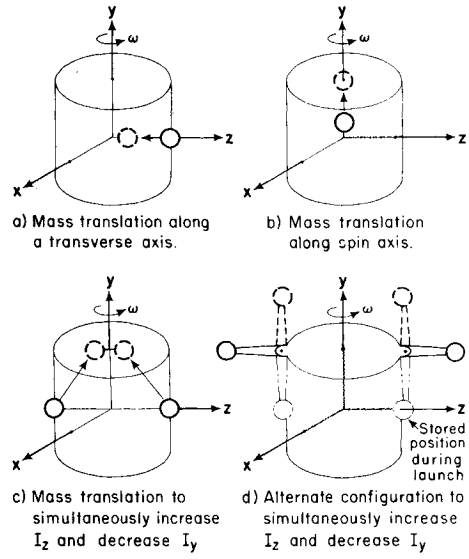

Fig. 1 Various configurations for a satellite inversion system (solid outline of control mass is position in normal operation).

The most straightforward method of inverting a spin-stabilized satellite is by applying a torque electromagnetically or by mass expulsion, but the large angular impulse required to turn the angular momentum vector through 180° makes this approach unattractive if inversion is to be done on a regular basis. For example, it would take about 5 lb of H_2O_2 (Specific Impulse = 160 sec) to invert a spin-stabilized satellite having a moment of inertia of 80 slug-ft^2 about the spin axis, a spin rate of 100 rpm, and a 25¼ in. radius for the jets. (System inefficiencies are ignored.)

An alternate approach is to allow the momentum vector to remain fixed in inertial space, but to cause the satellite to invert itself by proper manipulation of its moments of inertia.[1] With this technique, the spacecraft ends up rotating in the opposite direction than if precession were used, but this should normally be of no consequence.

If a rigid body rotates about its axis of maximum or minimum moment of inertia, the rotation is stable. On the other hand, if it rotates about the principal axis of intermediate moment of inertia, the rotation is unstable. In view of this, inversion may be accomplished in the following manner: with the satellite spin-stabilized about **y**, its axis of maximum moment of inertia, a mass is moved in a manner that causes 1) a slight rotation of principal axes **x**, **y**, and **z** with respect to the spacecraft so that **y** no longer coincides with the momentum vector, being offset from it by the angle α_o, and 2) a change in ratios of the principal moments of inertia so that **y** is now the principal axis of intermediate moment of inertia, with I_z just slightly greater than I_y. The unstable spacecraft will then proceed to invert itself. When it has tilted as far as it is going to (almost 180°), the control mass is returned to its original position, and the inverted spacecraft will again be spinning in a stable manner. The small amount of nutation caused by the maneuver can be readily eliminated by a nutation damper.

If we define the inversion maneuver as beginning at the completion of the control mass movement, it is completely described by Euler's dynamical equations for a rigid body,

$$I_x d\omega_x/dt + (I_y - I_z)\omega_y\omega_z = 0$$

$$I_y d\omega_y/dt + (I_z - I_x)\omega_z\omega_x = 0$$

$$I_z d\omega_z/dt + (I_x - I_y)\omega_x\omega_y = 0$$